

Dynamics of vortex glass phase in strongly type II superconductors

Qing-Hu Chen^{1,2,3}

¹ *CSTCMP and Department of Physics, Zhejiang Normal University, Jinhua 321004, P. R. China*

² *Department of Physics, Zhejiang University, Hangzhou 310027, P. R. China*

³ *Computational Materials Science Center, National Institute for Materials Science, Tsukuba 305-0047, Japan*

(Dated: August 15, 2021)

Dynamics of vortices in strongly type-II superconductors with strong disorder is investigated within the frustrated three-dimensional XY model. For two typical models in [Phys. Rev. Lett. **91**, 077002 (2003)] and [Phys. Rev. B **68**, 220502(R) (2003)], a strong evidence for the finite temperature vortex glass transition in the unscreened limit is provided by performing large-scale dynamical simulations. The obtained correlation length exponents and the dynamic exponents in both models are different from each other and from those in the three-dimensional gauge glass model. In addition, a genuine continuous depinning transition is observed at zero temperature for both models. A scaling analysis for the thermal rounding of the depinning transition shows a non-Arrhenius type creep motion in the vortex glass phase, contrarily to the recent studies.

PACS numbers: 74.25.Qt, 74.72.-h, 74.40.+k

I. INTRODUCTION

The application of superconductors crucially depends on the high electric current density without dissipation. However, the resistivity would always be nonzero even in the presence of pinning centers. This conventional picture has been changed with the discovery of high- T_c superconductors[1] and the progress in random field systems[2]. Similar to the spin-glass system, Fisher et al suggested that, for strong disorder, the system freezes into a genuine thermodynamic amorphous vortex glass (VG) phase with some kind of glassy long-range orders[3, 4]. The VG phase in strongly type II superconductors has attracted considerable attentions both experimentally and theoretically[5] during the past more than one decades. It is of practical significance that the VG phase is a true superconducting state with a vanishing linear resistivity by diverging energy barriers. On the fundamental side, it is closely related to an important class of phenomena in condensed matter physics, such as spin glasses, random field systems[2], and charge-density waves in solids[6].

The evidences to support the existence of a VG phase have been reported in many experiments by means of the dynamic scaling of the measured current-voltage (IV) data[7]. However, Strachan et al. have shown that a perfect collapse of the IV data is not the sufficient evidence for a VG transition [8], since the critical temperature and the scaling exponents are not uniquely determined by this dynamic scaling.

Theoretically, the XY gauge glass model[9, 10, 11, 12] has been extensively employed to study the VG transition. The values for the critical exponents are similar to those obtained in some experiments [7]. However, lacking some of properties and symmetries due to the absence of net magnetic fields, it is questioned to be a model of disordered superconductors in an applied field[13, 14, 15, 16, 17]. Some realistic models have then been proposed recently, but the conclusions were quite

contradictory. Continuous finite temperature VG transitions have been given by most models with various critical exponents. It was also observed that the VG phase disappears if the screening of the vortex interaction due to the gauge field fluctuation is included[18]. The simulation of the London-Langevin model suggested no VG phase[19].

Among all vortex models, the disordered three-dimensional (3D) XY model with net magnetic fields has provided both equilibrium and dynamical vortex phase diagrams in Type-II superconductors with weak disorder [20, 21]. The low field (weak disorder) low temperature phase is in general regarded as a dislocation-free Bragg glass with a quasi-long-range order[20], which was observed directly in a neutron experiment[22]. Several dynamical simulations on the vortex matter with rather low fields for weak disorder have been performed in this model[21, 23, 24]. By a anisotropic frustrated 3D XY model with strong disorder in the coupling constants, Olsson [14] provided evidence for the VG transition in the unscreened limit. The correlation length exponent $\nu = 1.5 \pm 0.3$ was obtained, consistent with the 3D gauge glass universality. Within an isotropic model with different choice of strong random-coupling distribution, Kawamura [15] reported similar results for the VG transition independently. Although the obtained value $\nu = 1.2 \pm 0.3$ is slightly smaller, which within the error bar also suggests a common universality with the 3D gauge glass model. However, it was found later that a convincing scaling collapse for helicity modulus could not be achieved in Kawamura's model[16], possibly due to the small effective randomness in the small system accessed. Furthermore, to the best of our knowledge, the dynamical study in the frustrated 3D XY model with strong disorder is so far lacking, which is however more relevant to experiments in the context of VG transitions.

In this paper, based on resistively-shunted-junction dynamics, we perform large scale dynamical simulations on the frustrated 3D XY models for two typical sets of pa-

rameters in Refs. [14, 15]. The glass transition temperatures and the critical exponents are estimated based on the simulated IV data. The depinning transition at zero-temperature and creep motion far below the glass transition temperature are also studied. The rest of the paper is organized as follows. Sec.II describes the models and dynamic method. In Sec. III and Sec. IV, the main results for the VG transition, the depining and creep motion of vortices are presented, and some discussions are also carried out. Finally, a short summary is given in the last section.

II. MODEL

The frustrated 3D XY model on a simple cubic lattice is given by [14, 15]

$$H = - \sum_{\langle ij \rangle} J_{ij} \cos(\phi_i - \phi_j - A_{ij}), \quad (1)$$

where ϕ_i specifies the phase of the superconducting order parameter on site i , $A_{ij} = (2\pi/\Phi_0) \int_i^j \mathbf{A} \cdot d\mathbf{l}$ with \mathbf{A} the magnetic vector potential of a field $\mathbf{B} = \nabla \times \mathbf{A}$ along the z axis, J_{ij} represents the random coupling distribution. The average number of vortex lines per plaquette is denoted by $f = l^2 B/\Phi_0$, where l is the grid spacing in the xy plane and Φ_0 is the flux quantum. We choose two typical sets of parameters used by Olsson[14] and Kawamura[15]. For convenience, the models with these parameters are called Models I and II respectively. In Model I, the random pinning potential is introduced in the coupling strength in the xy plane $J_{ij} = J_0(1 + p\epsilon_{ij})$, where ϵ_{ij} 's are independently Gaussian distributed with zero mean and unit variance, p represents the pinning strength. The coupling between the xy planes is $J_z = J_0/\Gamma^2$, (Γ is the anisotropy constant). We typically choose $p = 0.4$ which models strong pinning strength, $1/\Gamma^2 = 1/40$, and $f = 1/5$. Simulations of Model I are performed with system size $L_{xy} = 100, L_z = 60$ satisfying $L_{xy}/L_z = 5/3$, much too larger than those in Ref. [14]. In Model II, the quenched randomness is put in the coupling constant J_{ij} in all directions, which is distributed uniformly on the interval $[0, 2J_0]$. The filling factor is chosen to be $f = 1/4$. The present simulations of Model II are performed with the system size $L = 64$ for all directions, considerably larger than those in Ref. [15].

The Resistivity-Shunted-Junction dynamics is incorporated in simulations, which can be described as

$$\frac{\sigma \hbar}{2e} \sum_j (\dot{\phi}_i - \dot{\phi}_j) = -\frac{\partial H}{\partial \phi_i} + J_{\text{ext},i} - \sum_j \eta_{ij}, \quad (2)$$

where $J_{\text{ext},i}$ is the external current which vanishes except for the boundary sites. The η_{ij} is the thermal noise current with zero mean and a correlator $\langle \eta_{ij}(t)\eta_{ij}(t') \rangle = 2\sigma k_B T \delta(t-t')$. In the following, the units are taken of $2e = J_0 = \hbar = \sigma = k_B = 1$.

In the present simulation, a uniform external current I_x along x -direction is fed into the system, analogous to experiments[7]. The fluctuating twist boundary condition [25] is applied in the xy plane to maintain the current, and the periodic boundary condition is employed in the z axis. In the xy plane, the supercurrent between sites i and j is now given by $J_{i \rightarrow j}^{(s)} = J_{ij} \sin(\theta_i - \theta_j - A_{ij} - \mathbf{r}_{ij} \cdot \mathbf{\Delta})$, with $\mathbf{\Delta} = (\Delta_x, \Delta_y)$ the fluctuating twist variable and $\theta_i = \phi_i + \mathbf{r}_i \cdot \mathbf{\Delta}$. The new phase angle θ_i is periodic in both x - and y -directions. Dynamics of $\mathbf{\Delta}_\alpha$ can be then written as

$$\dot{\Delta}_\alpha = \frac{1}{L^3} \sum_{\langle ij \rangle_\alpha} [J_{i \rightarrow j}^{(s)} + \eta_{ij}] - I_\alpha, \alpha = x, y. \quad (3)$$

The voltage drop is $V = -L\dot{\Delta}_x$.

The above equations can be solved efficiently by a pseudo-spectral algorithm [21] due to the periodicity of phases in all directions. The time stepping is done using a second-order Runge-Kutta scheme with $\Delta t = 0.05$. The equilibration of the simulation should be ensured before the measurement. So most of our runs are typically $(4-8) \times 10^7$ time steps and the latter half time steps are for the measurements. The detailed procedure in the simulations was described in Ref. [21]. Our results are based on one realization of disorder. The present system size is much too larger than those reported in literature, it is expected to exist a good self-averaging effect. We have done two additional simulations with different realizations of disorder for further confirmations, and indeed observed quantitatively the same behavior. In addition, it is practically difficult to perform any serious disorder averaging for such a rather large system. Actually, the results from dynamic simulations on 3D XY model in the recent literature were also for a single disorder realization[21, 23, 24], mainly due to the large system simulated. For the data points presented in the following figures, the statistical errors are smaller or comparable to the symbol sizes.

III. VG PHASE TRANSITIONS

First, we study the VG phase transition in these two models. In Model I, the VG transition temperature T_g is estimated to be 0.123 ± 0.008 in equilibrium simulations[14]. The IV characteristics is simulated at temperatures ranged from 0.08 to 0.15, which must covers possible T_g . In the equilibrium simulations of Model II, Kawamura[15] obtained $T_g = 0.81$ by performing the finite-scaling analysis of the Binder ratio and the mean-square current. The similar simulations on Model II are performed at the temperatures ranged from 0.5 to 1.1, which also covers the possible T_g . In simulations on both models, we try to probe the system at currents as low as possible for each temperature. Figs. 1(a) and 1(b) present the resistivity $R = V/I$ as a function of current I at various temperatures for Models I and II, respectively. It is clear that, at lower temperatures, R tends to zero as

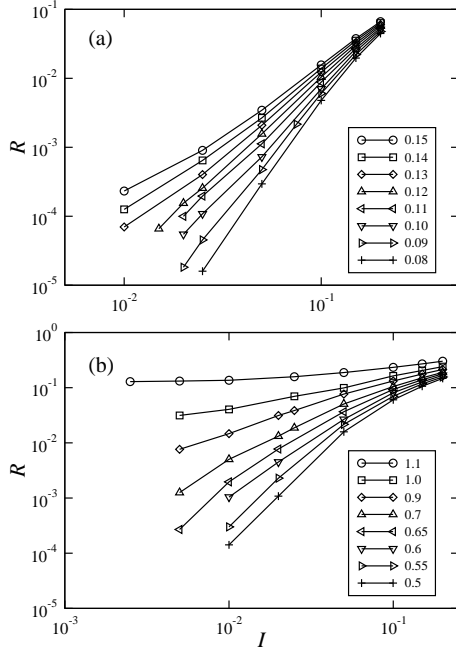


FIG. 1: Current-resistivity curves at various temperatures for (a) Model I and (b) Model II

the current decreases, which follows that there is a true superconducting phase with zero linear resistivity. While R tends to a finite value at higher temperatures, corresponding to an Ohmic resistivity in the vortex liquid. These observations provide a evidence of the existence of the VG phase in both models.

Assuming that the vortex glass transition is continuous and characterized by the divergence of the characteristic length and time scales $t \sim \xi^z$ (z is the dynamic exponent), Fisher, Fisher, and Huse [4] proposed the following dynamic scaling ansatz to analyze the glass transition from a vortex liquid with ohmic resistance to a superconducting glass state,

$$TR\xi^{1-z} = \Psi_{\pm}(I\xi^2/T). \quad (4)$$

where $\xi \propto |T/T_g - 1|^{-\nu}$ is the correlation length which diverges at the transition. $\Psi(x)$ is a scaling function with the + and - signs corresponding to $T > T_g$ and $T < T_g$. Eq. (4) was often used to scale measured IV data experimentally[7].

Right at T_g , the RI curve should show a power law behavior $R \propto I^{-\alpha}$ where $\alpha = (z - 1)/2$, which provides a convexity-concavity criterion to identify the VG transition temperature as well as the dynamic exponent z . As shown in Figs. 1(a) for Model I that the value of T_g is in between (0.12 - 0.13), because in the low current regime the RI curves show convexity below $T = 0.12$ and concavity above $T = 0.13$. The RI curves at other temperatures within (0.12, 0.13) can be obtained by interpolations. The temperature at which the RI curve most close to the power law behavior is regarded as T_g and the RI power law exponent at T_g gives the dynamic

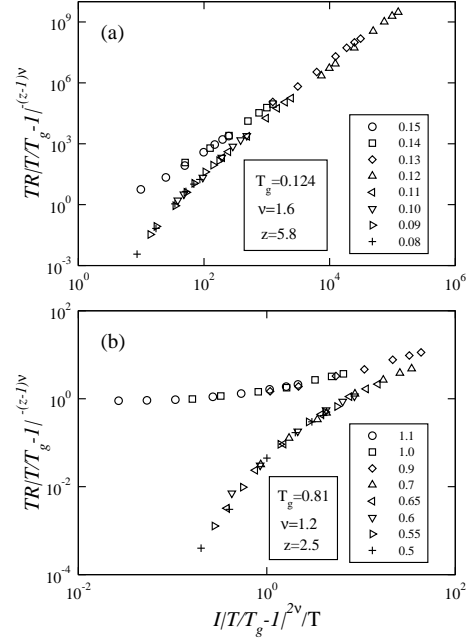


FIG. 2: Dynamic scaling of IV data at various temperatures for (a) Model I and (b) Model II

exponent z . The error bars are estimated by obvious deviation from the power law behavior. In this way, for Model I, we obtain $T_g = 0.124 \pm 0.002$ and $z = 5.8 \pm 0.3$. The value of T_g is consistent with that in equilibrium simulations[14]. By the similar method, for Model II, we get $T_g = 0.81 \pm 0.01$, $z = 2.5 \pm 0.2$. Interestingly, the present value of T_g in Model II agrees well with that in equilibrium Monte Carlo simulations by Kawamura[15].

Once T_g and z have been estimated, we can examine the IV data at different temperatures by the dynamical scaling. Fig. 2(a) shows that the data collapses well according to Eq. (4) if using the correlation length exponent $\nu = 1.6 \pm 0.1$. The error bar is estimated by tuning the value of ν until the collapse becomes poor evidently. The value of ν is very close to $\nu = 1.5 \pm 0.3$ obtained in Ref. [14] through equilibrium Monte Carlo simulations of Model I. Also as indicated in Fig. 2(b) that, using $\nu = 1.2 \pm 0.1$, an excellent collapse according to Eq. (4) is achieved. The value of ν also agrees quite well with $\nu = 1.2 \pm 0.3$ estimated in an equilibrium Monte Carlo simulations of Model II[15]. Interestingly, although the values of ν in both Models lie in the range [1.0 - 2.0] usually observed experimentally [7], they are close to but different from each other. Since the present two models involve different symmetries (anisotropy) and different disorders included, in our opinion, it is not unlikely that they represent different universality classes.

It should be mentioned that the present analysis method for the VG phase transition is not essentially inconsistent with that described in Ref. [8]. We also think that only the perfect collapse of the IV data is not a sufficient evidence for a VG transition, so we use

the convexity-concavity criterion to identify T_g and determine z before performing the dynamic scaling.

In equilibrium Monte Carlo simulations of Model II, some quantities failed to provide good scaling[16]. The helicity modulus was used in the finite size scaling analysis of the VG phase transitions in both models[14, 16], a nice scaling is obtained in Model I, but scaling fails applied to Model II for data in system sizes $L \leq 20$. The collapse of the transverse helicity modulus with poor quality gives $T_g = 0.63$, $\nu = 1.5$, which differed significantly from those in Ref. [15]. More seriously, it was impossible to collapse the data for the parallel helicity modulus. It has been observed[20] that the correct behavior required a great flexibility of the field induced vortex lines, which could be obtained either with a very large size or with weak interplane coupling along the field direction. For the isotropic system in Model II, the possible way to get a convincing scaling collapse of some quantities is to enlarge the systems. In the present large scale dynamical simulations, an excellent collapse of the IV data in the dynamic scaling is indeed achieved.

The exponents ν in the present two models are close to $\nu = 1.39 \pm 0.20$ evaluated by Olson and Young[10], but different from the recent more accurate result $\nu = 1.39 \pm 0.05$ obtained by Katzgraber and Campbell [11] in the 3D gauge glass model, suggesting that they are not in the same universality class. It follows that the difference in the quenched randomness and the introduction of net fields may change the static critical properties of the VG transitions.

The dynamic exponents z in these two models are found to be quite different. The exponent z in Model I is high, in the range $[4.0 - 6.0]$ usually measured in experiments[7], in Model II is however considerably low. Note that small values of the exponent z were also reported[26]. In addition, both exponents z in Models I and II can not fall even within the error bar of that in the 3D gauge glass model, which were estimated to be $z = 4.2 \pm 0.6$ in Ref. [10] and $z = 4.7 \pm 0.1$ in Ref. [11], although the exponent z in Model I seems to be more close. It is possible that the disorder in the coupling constant along the field direction in Model II reduces the effective pinning strength [16], leading to a small IV power law exponent at the VG transition. It is not expected that enlarging the system size further along the field direction would change the dynamic exponent z essentially. Nevertheless, the reason for the small value of z in Model II is not fully understood at the present stage, the further investigation is clearly called for.

IV. DEPINING AND CREEP

With the VG phase in hand, we then study the depinning and creep motion of the vortices in this phase for both models. To study the depinning transition at zero temperature, we start from high currents with random initial phase configurations. The current is then

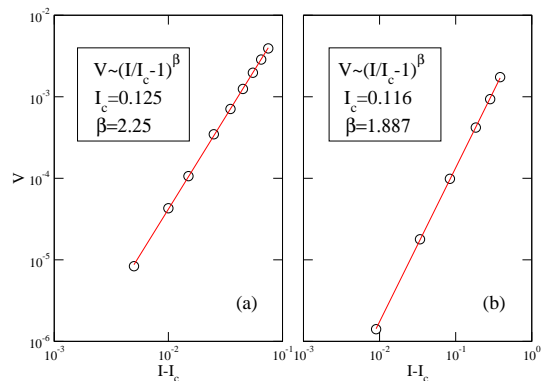


FIG. 3: Log-log plots of IV data at zero-temperatures for (a) Model I and (b) Model II.

lowered step by step. The steady-state phase configurations obtained at higher currents are chosen to be the initial phase configurations of the lower currents in the next step. It becomes more difficult to measure the voltage with the lower currents. In the vicinity of the critical current, a huge amount of the computer time is consumed to get accurate results. Fig. 3 exhibits the IV characteristics at $T = 0$ for both models. Interestingly, we observe continuous depinning transitions with unique depinning currents[27], which can be described as $V \propto (I - I_c)^\beta$ with $I_c = 0.125 \pm 0.001$, $\beta = 2.25 \pm 0.02$ for Model I and $I_c = 0.116 \pm 0.002$, $\beta = 1.887 \pm 0.01$ for Model II. Note that the depinning exponents for both models are greater than 1, consistent with the mean field studies on charge-density wave models[27]. The depinning exponent is model dependent, possibly due to the different realizations of the disorder.

At low temperatures, the IV curves are rounded near the zero-temperature critical current due to thermal fluctuations. An obvious crossover between the depinning and creep motion can be observed around I_c for both models at the lowest accessible temperatures. In order to address the thermal rounding of the depinning transition, Fisher[27] first suggested to map this system to the ferromagnet in fields where the second-order phase transitions occur. This mapping was later extended to the random-field Ising model[28] and flux lines in type-II superconductors[29]. If the voltage is identified as the order parameter, the current and temperature are identified as the inverse temperature and the field in the ferromagnetic system respectively, analogous to the second-order phase transitions, a scaling relation among the voltage, current, and temperature in the present model should satisfy the form

$$V(T, I) = T^{1/\delta} S[T^{-1/\beta\delta}(1 - I_c/I)], \quad (5)$$

where $S(x)$ is a scaling function.

It is implied that right at $I = I_c$ the voltage shows a power-law behavior $V(T, I = I_c) \propto T^{1/\delta}$ and the critical exponent $1/\delta$ can be determined. The log-log $V - T$ curves are plotted in Fig. 4 (a) and (b) at three cur-

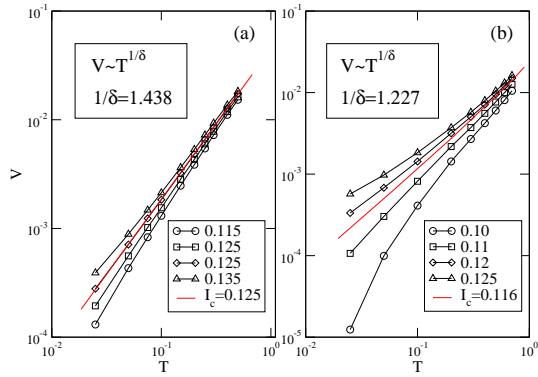


FIG. 4: Log-log plots of $V - T$ at three currents around I_{c0} for (a) Model I and (b) Model II.

rents for Models I and II. In Fig. 4(a), we can see that the critical current is between 0.115 and 0.135. The values of voltage at other currents within (0.115, 0.135) can be evaluated by quadratic interpolations. The deviation of voltage from the power law is calculated as the square deviations. The current at which the square deviation is minimum is defined as the critical current $I_c = 0.125 \pm 0.02$, consistent with those obtained at zero temperature. The temperature dependence of voltage at the critical current is also plotted in Fig. 4(a). The slope of this curve yields $1/\delta = 1.438 \pm 0.004$. The similar analysis in Fig. 4(b) yields $I_c = 0.116 \pm 0.02$ for Model II, consistent with that extracted from the zero-temperature simulation. The exponent $1/\delta = 1.227 \pm 0.003$ is achieved by fitting the $V - T$ curve in the low temperature regime at the critical current.

With the critical exponent δ and the critical current I_c , we can adjust the depinning exponent β to achieve the best data collapse according to the scaling relation Eq. (5) for $I \leq I_c$. In Fig. 5 (a) and (b), a perfect collapse of the IV data at various temperatures below T_g is shown with $\beta = 2.25 \pm 0.01$ for Model I and 1.89 ± 0.01 for Model II. The values of β estimated from low temperature creep motion are in excellent agreement with those derived at $T = 0$ depinning transition. Moreover, the scaling function with the form $V \propto T^{1/\delta} \exp[A(1 - I/I_c)/T^{\beta\delta}]$ is derived in the creep regime for both models, which are also demonstrated in the legends of Figs. 5 (a) and (b). Note that the product of the two exponents $\beta\delta$ describes the temperature dependence of the creeping law. Interestingly, $\beta\delta \simeq 1.56$ for Model I and $\beta\delta \simeq 1.54$ for Model II are obtained, both deviate from unity, demonstrating that the creep law is a non-Arrhenius type. The values of $\beta\delta$ in both models are close to $3/2$, which may motivate a further analytical work. In our opinion, it is not a coincidence that they are in the same universality class in the depinning transition.

In a recent study of the depinning and creep motion of the flux line system in type-II superconductors[29], by simulations of overdamped London-Langevin model, Luo and Hu observed an Arrhenius law for the creep motion

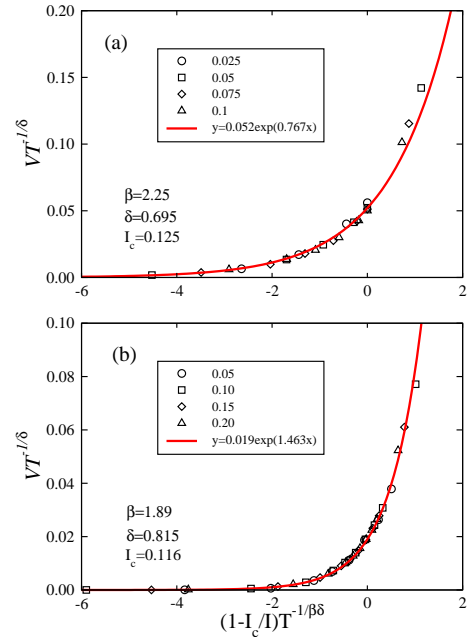


FIG. 5: Scaling plot of the IV data at various temperatures below T_g for (a) Model I and (b) Model II.

with a linearly suppressed energy barrier for strong pinning [29], inconsistent with the present study for strong disorder. It is worth noting that, in the London-Langevin model, the stable VG phase with the freezing of disordered vortex matter is not found[19] and instead the vortices freeze like a window glass, called vortex molasses scenario. In the framework of the frustrated 3D XY model, the existence of a stable VG phase is well established in the unscreened limit in the present dynamical simulations, as well as in previous equilibrium Monte Carlo simulations[14, 15, 16]. In the real strongly type-II superconductors, the screening induced rounding of the sharp VG transition is only a weak effect, and only visible at temperatures very close to T_g . The present good scaling behavior in the creep motion is just observed far below T_g . We believe that the different nature of the phase in the London-Langevin model with strong pinning [29] and the VG phase in the present two models is the possible reason for the discrepancy. In addition, the Anderson-Kim creep law [32] is realized in the London-Langevin model with strong pinning [29], which may suggest that it is applicable to strong flux pinning in the conventional low T_c superconductors rather than a VG phase with random point pins.

The non-Arrhenius type creep behaviors have been also observed in charge-density waves with the mean-field result $\beta\delta = 2/3$ [30], the 3D random-field Ising model with $\beta\delta \approx 3/2$ [28], (1+1) elastic interface with $\beta\delta \approx 2$ [31], and the flux line system in type-II superconductors for weak pinning in a Bragg glass phase with $\beta\delta \approx 3/2$ [29]. It is surprising to note that the present combined exponent $\beta\delta \approx 3/2$ in the frustrated 3D XY model for strong disorder

der is close to that in the 3D London-Langevin model for weak-pinning [29]. In the London-Langevin model of a fixed number of interacting particles, the vortex loop between the planes perpendicular to the field is absolutely excluded, while in the present 3D XY models, the vortex loops between the planes can be induced by both thermal activations and the quenched disorder. So we argue that the disorder strengths in these two different kinds of models are hard to compare. Interestingly, the combined depinning exponent $\beta\delta \approx 3/2$ was also observed in the depinning of domain walls in the 3D random-field Ising model [28], possibly suggesting a universal rule in high dimensional elastic systems. Whereas the present results are different from recent results for (1+1) elastic interfaces in a disorder medium[31], possibly owing to the two-dimensional nature in the latter. Further work is needed in order to clarify these observations.

Note that the depinning of Bragg glass phase has been studied recently by Olsson using essentially the same model as Model I with a rather weak field $f = 1/45$ [23]. The IV characteristics showed a unexpected behavior with a critical current that separates the creep region with an immeasurably low voltage at $I < I_c$ from a region with $V \propto (I - I_c)$. This behavior is not observed in the present two models, possibly owing to the strong disorder and high fields. Their study together with the present one constitute a complementary picture for the depinning in the disordered 3D XY model with net fields.

V. SUMMARY

We have performed large scale dynamical simulations on the frustrated 3D XY models for strong disorder with

two typical sets of parameters used in recent literature, within the resistively-shunted-junction dynamics. We first use the convexity-concavity criterion to identify T_g and determine z , then perform the dynamic scaling on the simulated IV data. Adjusting the single parameter ν , a perfect collapse of IV data is achieved for both cases, providing a evidence of the VG transition in the unscreened limit convincingly. Although the obtained correlation length exponents agree with the previous ones within error bars in equilibrium simulations, they are close to but different from each other, suggesting different universality class. New dynamic exponents are found to be parameter dependent. Both the static and dynamic exponents are different from the recent accurate results in the 3D gauge glass model. The nonlinear dynamical response far below the glass transition is studied systematically. A non-Arrhenius type creep motion in the VG phase is observed, contrarily to the recent studies of the flux line system with strong pinning. The combined depinning exponent $\beta\delta = 3/2$ is consistent with those in the 3D random-field Ising model and the flux line system with weak pinning, suggesting the common universality class in the depinning transitions in these systems.

VI. ACKNOWLEDGEMENTS

The author acknowledges useful discussions with X. Hu, X. G. Li, L. H. Tang, and H. H. Wen. The present simulations were partially performed on SR11000 (HITACHI) at NIMS, Japan. This work was supported by National Natural Science Foundation of China under Grant No. 10574107, PNCET and PCSIRT in University in China, National Basic Research Program of China (Grant No. 2006CB601003).

-
- [1] G. Blatter, M. V. Feigel'man, V. B. Geshkenbein, A. I. Larkin and V. M. Vinokur, *Rev. Mod. Phys.* **66**, 1125 (1994).
 - [2] P. Young, *Spin Glass and Random fields* (World Scientific, Singapore, 1998).
 - [3] M. P. A. Fisher, *Phys. Rev. Lett.* **62**, 1415 (1989).
 - [4] D. Fisher, M. P. A. Fisher and D. Huse, *Phys. Rev. B* **43**, 130 (1991).
 - [5] T. Nattermann and S. Scheidl, *Adv. Phys.* **49**, 607(2000).
 - [6] G. Grüner, *Rev. Mod. Phys.* **60**, 1129 (1988).
 - [7] R. H. Koch, V. Foglietti, W. J. Gallagher, G. Koren, A. Gupta and M. P. Fisher, *Phys. Rev. Lett.* **63**, 1511 (1989); R. Koch, V. Foglietti and M. P. A. Fisher, *Phys. Rev. Lett.* **64**, 2586 (1990); A. M. Petrean, L. M. Paulius, W.-K. Kwok, J. A. Fendrich and G. W. Crabtree, *Phys. Rev. Lett.* **84**, 5852 (2000); U. Divakar, A. J. Drew, S. L. Lee, R. Gilardi, J. Mesot, F. Y. Ogrin, D. Charalambous, E. M. Forgan, G. I. Menon, N. Momono, M. Oda, C. D. Dewhurst and C. Baines, *Phys. Rev. Lett.* **92**, 237004 (2004); J. E. Villegas and J. L. Vicent, *Phys. Rev. B* **71**, 144522(2005).
 - [8] D. R. Strachan, M. C. Sullivan, P. Fournier, S. P. Pai, T. Venkatesan and C. J. Lobb, *Phys. Rev. Lett.* **87**, 067007(2001); I. L. Landau and H. R. Ott, *Phys. Rev. B* **65**, 064511 (2002).
 - [9] D. A. Huse and H. S. Seung, *Phys. Rev. B* **42**, R1059 (1990); J. D. Reger, T. A Tokuyasu, A. P. Young and M. P. A. Fisher, *Phys. Rev. B* **44**, 7147 (1991).
 - [10] T. Olson and A. P. Young, *Phys. Rev. B* **61**, 12467(2000)
 - [11] H. G. Katzgraber and I. A. Campbell, *Phys. Rev. B* **69**, 094413 (2004).
 - [12] J. M. Kosterlitz and N. Akino, *Phys. Rev. Lett.* **81**, 4672 (1998).
 - [13] A. Vestergren, J. Lidmar and M. Wallin , *Phys. Rev. Lett.* **88**, 117004 (2002).
 - [14] P. Olsson, *Phys. Rev. Lett.* **91**, 077002 (2003).
 - [15] H. Kawamura, *Phys. Rev. B* **68**, 220502(R) (2003).
 - [16] P. Olsson, *Phys. Rev. B* **72**, 144525 (2005).
 - [17] J. Lidmar, *Phys. Rev. Lett.* **91**, 097001(2003); Rodriguez, *Phys. Rev. B* **69**, 100503 (R) (2004).
 - [18] H. S. Bokil and A. P. Young, *Phys. Rev. Lett.* **74**, 3021 (1995); J. Kisker and H. Rieger, *Phys. Rev. B* **58**, R8873 (1998); H. Kawamura, *J. Phys. Soc. Jpn.* **69**, 29 (2000).
 - [19] C. Reichhardt, A. V. Otterlo and G. T. Zimanyi, *Phys.*

- Rev. Lett. **84**, 1994 (2000); S. Bustingorry, L. F. Cugliandolo and D. Dominguez, Phys. Rev. Lett. **96**, 027001(2006).
- [20] Y. Nonomura and X. Hu, Phys. Rev. Lett. **86**, 5140(2001); P. Olsson and S. Teitel, Phys. Rev. Lett. **87**, 137001(2001).
- [21] Q. H. Chen and X. Hu, Phys. Rev. Lett. **90**, 117005(2003).
- [22] T. Klein, I. Joumard, S. Blanchard, J. Marcus, R. Cubitt, T. Giamarchi and P. Le Doussal, Nature (London) **413**, 404(2001).
- [23] P. Olsson, Phys. Rev. Lett. **98**, 097001 (2007)
- [24] A. D. Hernández and D. Domínguez, Phys. Rev. Lett. **92**, 117002 (2004)
- [25] Q. H. Chen, L. H. Tang, and P. Q. Tong, Phys. Rev. Lett. **87**, 067001(2001); L. H. Tang and Q. H. Chen, Phys. Rev. B **67**, 024508 (2003).
- [26] P. Gammel, L. Schneemeyer, and D. Bishop, Phys. Rev. Lett. **66**, 953 (1991); N.-C. Yeh, D. S. Reed, W. Jiang, U. Kriplani, F. Holtzberg, A. Gupta, B. D. Hunt, R. P. Vasquez, M. C. Foote and L. Bajuk, Phys. Rev. B **45**, 5654(1992).
- [27] D. S. Fisher, Phys. Rev. Lett. **50**, 1486 (1983); Phys. Rev. B **31**, 1396 (1985).
- [28] L. Roters, A. Hucht, S. Lubeck, U. Nowak and K. D. Usadel, Phys. Rev. E **60**, 5202 (1999).
- [29] M. B. Luo and X. Hu, Phys. Rev. Lett. **98**, 267002(2007).
- [30] O. Narayan and D. S. Fisher, Phys. Rev. B **46**, 11520 (1992); A. A. Middleton, Phys. Rev. B **45**, 9465 (1992).
- [31] S. Bustingorry, A. B. Kolton and T. Giamarchi, Europhys. Lett. **81**, 26005 (2008).
- [32] P. W. Anderson and Y B. Kim, Rev. Mod. Phys. **36**, 39 (1964).